# Multiplexed Real-Time Polymerase Chain Reaction on a Digital Microfluidic Platform

**ARTICLE** *in* ANALYTICAL CHEMISTRY · FEBRUARY 2010

Impact Factor: 5.64 · DOI: 10.1021/ac902510u · Source: PubMed

Published in final edited form as:
*Anal Chem*. 2010 March 15; 82(6): 2310–2316. doi:10.1021/ac902510u.

# Multiplexed Real-Time Polymerase Chain Reaction on a Digital Microfluidic Platform

**Zhishan Hua**[1], **Jeremy L. Rouse**[1], **Allen E. Eckhardt**[1], **Vijay Srinivasan**[1], **Vamsee K. Pamula**[1], **Wiley A. Schell**[2], **Jonathan L. Benton**[2], **Thomas G. Mitchell**[3], and **Michael G. Pollack**[1,*]

[1] Advanced Liquid Logic Inc., Research Triangle Park, North Carolina

[2] Division of Infectious Diseases, Department of Medicine, Duke University Medical Center, Durham, North Carolina

[3] Department of Molecular Genetics and Microbiology, Duke University Medical Center, Durham, North Carolina

## Abstract

This paper details the development of a digital microfluidic platform for multiplexed real-time polymerase chain reactions. Liquid samples in discrete droplet format are programmably manipulated upon an electrode array by the use of electrowetting. Rapid PCR thermocycling is performed in a closed-loop flow-through format where for each cycle the reaction droplets are cyclically transported between different temperature zones within an oil-filled cartridge. The cartridge is fabricated using low-cost printed-circuit-board technology and is intended to be a single-use disposable device. The PCR system exhibited remarkable amplification efficiency of 94.7%. To test its potential application in infectious diseases, this novel PCR system reliably detected diagnostic DNA levels of methicillin-resistant *Staphylococcus aureus* (MRSA), *Mycoplasma pneumoniae*, and *Candida albicans*. Amplification of genomic DNA samples was consistently repeatable across multiple PCR loops both within and between cartridges. In addition, simultaneous real-time PCR amplification of both multiple different samples and multiple different targets on a single cartridge was demonstrated. A novel method of PCR speed optimization using variable cycle times has also been proposed and proven feasible. The versatile system includes magnetic bead handling capability, which was applied to the analysis of simulated clinical samples that were prepared from whole blood using a magnetic bead capture protocol. Other salient features of this versatile digital microfluidic PCR system are also discussed, including the configurability and scalability of microfluidic operations, instrument portability and substrate-level integration with other pre- and post-PCR processes.

### Keywords

digital microfluidics; real-time PCR; electrowetting; droplets; *Candida albicans*; *Mycoplasma pneumoniae*; *Staphylococcus aureus*; molecular diagnostics

*Corresponding Author. Mailing address: Advanced Liquid Logic, Inc., PO Box 14025, Research Triangle Park, NC 27709. Phone: (919) 287-9010. Fax: (919) 287-9011. mpollack@liquid-logic.com.

## INTRODUCTION

As a standard technique to selectively and exponentially amplify trace amounts of DNA, the polymerase chain reaction (PCR) has revolutionized the field of modern biology and has become a routine analytical tool in diagnostics, forensics, and life science research. In recent years, the concept of miniaturizing and automating PCR systems through microfluidics and advanced microfabrication techniques has attracted a great deal of attention because of the potential to dramatically improve the speed, portability, cost and performance of conventional PCR assays.[1,2] A variety of microfluidic systems have been successfully developed to implement microchip PCR, and thermocycling in these systems is generally achieved using one of two distinct schemes. The PCR mix is either thermocycled statically in a microchamber,[3–5] or continuously transported in a microchannel that traverses alternating temperature zones.[6–8] In both cases, rapid thermal cycling can be achieved by minimizing the total thermal mass which must be heated or cooled in each cycle. In static systems this has been accomplished using engineered microstructures such as thin-film heaters[3] and thermal isolators[9] to minimize the heat capacity of the heater-reaction system. Another static approach achieved extremely rapid thermal cycling using infrared radiation to selectively heat a reaction mixture without heating the surrounding chamber.[5] Continuous-flow PCR formats circumvent the need for repeated heating and cooling of the reaction chamber by moving the sample through alternating temperature zones, thus greatly reducing the cycled thermal mass while providing simplified temperature control. However, the relatively large surface-to-volume ratio makes continuous-flow PCR devices vulnerable to surface-induced reaction inhibition and cross-contamination. These issues can be mitigated by confining the PCR to a discrete microdroplet or plug surrounded by an immiscible carrier fluid.[10,11] The use of discrete droplets also enables much higher throughputs and improves sensitivity, in some cases enabling the detection of single copy templates.[12,13] However, the continuous-flow nature of these droplet-based PCR systems possess some inherent drawbacks, including large device footprints, fixed cycle numbers and inflexible dwell times (or dwell ratios) in the different temperature zones.

Several research groups have adapted the traditional continuous-flow format to bidirectional-flow or circular-flow schemes to achieve more flexible control of cycle numbers and dwell times.[14–20] The footprints of these devices have also been reduced considerably through the use of closed-loop flow formats. In these devices, the transportation of individual reaction droplets or plugs was achieved using mechanisms such as external magnets,[14–16] pumps,[17–19] or membrane actuators.[20] However, these methods provide only limited capability for the controllable manipulation of discrete liquid droplets. Scaling, multiplexing, and the integration of additional processing steps, such as sample preparation, are difficult to implement in these systems.

More recently, electrowetting has emerged as a convenient and robust technique to manipulate discrete droplets of a variety of liquids ranging from water to human physiological fluids.[21–28] In a typical electrowetting device, the droplets are sandwiched between an electrically grounded top plate and a bottom plate containing an array of individually addressable electrodes.[23] The interior surfaces of both plates are coated with a hydrophobic material and the intervening space is typically filled with an immiscible non-conductive fluid to prevent evaporation of the droplets and to facilitate their transport across the chip surfaces. The complete assembly consisting of the top-plate, bottom-plate, stand-off/gasket layer and loading ports is referred to as a “chip” or “cartridge”. Activation of a surface electrode within the cartridge results in a local reduction of the droplet-surface interfacial tension which increases the wettability of the liquid droplet on the hydrophobic surface. Application of a voltage to an electrode adjacent to a droplet (with other electrodes grounded) creates an energy gradient on the surface which causes the droplet to move and

align itself with the energized electrode. Through successive stepwise alignments droplets can be rapidly and programmatically transported along any path of contiguous electrodes. Using similar schemes of voltage switching, a complete kit of microfluidic operations including transporting, merging, splitting, mixing and dispensing of microdroplets can be implemented to enable the simultaneous and independent manipulation of multiple droplets.[23,24,29] Because the liquid droplets are discrete and are amenable to addressable and synchronous manipulation by a software program, this approach is often referred to as "digital microfluidics".[30,31] Recently, electrowetting-based digital microfluidics has been applied to implement a variety of miniaturized assays including immunoassays,[32] enzyme assays,[33] clinical chemistry,[28] proteomic sample preparation[34] and PCR.[32,35,36]

We present here an automated and self-contained multichannel digital microfluidic platform for multiplexed real-time PCR assays. The system is based on our previous implementation of DNA amplification using an electrowetting-enabled flow-through method, whereby thermocycling is accomplished by cyclically shuttling a droplet between two fixed temperature zones.[37,38] The system requires no pumps or valves for fluid manipulation, and features a disposable reaction cartridge fabricated using a low-cost printed-circuit-board (PCB) process. The compact and inexpensive system provides a high degree of flexibility enabling a wide range of methods, protocols and thermocycling conditions to be implemented on a single platform. The performance and functionality of this digital microfluidic PCR system is fully characterized and discussed in this paper.

## EXPERIMENTAL

### System Architecture

As shown in Figure 1A, the digital microfluidic PCR system comprises an instrument incorporating all of the required control and detection capabilities, and a disposable microfluidic cartridge in which sample processing and PCR takes place. The PCR cartridge is inserted into an instrument deck containing heaters and magnets, and communicates with the instrument through an electrical interface. All of the electronics and heaters are powered by a standard computer power supply contained in the instrument. The entire system is roughly the size of a shoebox, and may be linked to a personal computer through a USB.

### Electrical Control

Microfluidic control on the PCR cartridge is enabled by an electrical controller, which has a microprocessor and switching circuitry to deliver electrowetting actuation voltages (0--300 V) to 64 individually addressed channels. The controller includes an embedded microprocessor for downloading, storing and executing programs out of on-board memory and for operating peripheral devices such as heaters and detectors. The electrical interface between the instrument and the cartridge is made by spring-loaded connector pins aligned to copper contact pads on the PCB cartridge.

### Optical Detection

Fluorescence detection for real-time PCR is achieved using a custom-designed miniature fluorimeter module consisting of four independent and spatially separated channels. Each channel comprises a light emitting diode (RL3-B2030, SuperBrightLEDS, MO), a photodiode (S2386-18K, Hamamatsu, Japan), and a FITC filter set (Semrock, NY) along with a long-pass dichroic mirror. The fluorimeter module is mounted directly above the cartridge deck facing the annealing/extension zone of the PCR cartridge. The excitation source (475 nm peak wavelength) produces an illumination spot 500 μm in diameter which is focused and centered within specific "detection" electrodes (1.375 mm wide squares) on the chip. A lock-in amplifier is used to reject background signal from ambient light.

### Cartridge Deck Design

The cartridge deck is a plastic fixture with mechanical features designed to bring heaters, magnets and optics into alignment with specific areas on the cartridge. Cylindrical neodymium magnets (1/8″ D × 1/8″ H, KJ Magnetics, PA) are embedded at appropriate locations on the deck for the manipulation of paramagnetic beads in liquid samples. The deck is equipped with two aluminum heater bars (3.95″ L × 0.5″ W × 0.25″ H), each of which has 15-ohm resistors attached at each end of the underside of the bar to provide uniform heating. A miniature thermistor probe inserted into the center of the heater bar provides temperature measurement for feedback to a closed-loop PID controller contained within the instrument. The heater bar is aligned on the cartridge deck using positioning screws and supported by springs underneath to insure uniform and consistent thermal contact between the heater bar and the cartridge. The springs also serve to isolate the heater bars from the cartridge deck to avoid unwanted heat transfer. To calibrate the heating system, miniature thermocouples (Omega Engineering, CT) were inserted into the cartridge measuring the oil temperature. The steady-state temperature difference between the heater bar and the center of the droplet in the 60 °C and 95 °C zones were determined and an offset was applied correspondingly to the heater bar set point during PCR to accurately control the temperature inside the droplet. The two-temperature configuration described here may be expanded to three or more temperature zones by inserting additional heater bars in the cartridge deck.

### Cartridge Design and Manufacturing

The PCR cartridge consists of a PCB substrate (86 mm × 86 mm) containing the electrodes and electrical contact pads, and a glass cover plate containing the ground electrode and fluidic ports. The physical assembly and schematic of the cartridge are shown in Figure 1. The design contains four separate electrode loops traversing the two temperature zones. Each loop can accommodate a single droplet or a train of droplets thermocycled with programmably adjustable cycle numbers and dwell times. Each loop can be independently controlled, and each has a “detection” electrode in the extension/annealing zone, which is aligned to one of the illumination spots of the four-channel fluorimeter module. A total of eight chip reservoirs are provided for loading of DNA samples and PCR reagents. Droplets can be selectively dispensed from any reservoir and transported, split, mixed and reacted with other droplets on the adjacent electrode network to prepare the PCR droplets. Thermocycling is performed within the loops, which are controlled using a multiphase transporter design consisting of electrically connected set of electrodes that are activated together to enable synchronized clockwise or counter-clockwise rotation in each loop. This configuration minimizes the number of electrical contacts required while preserving a high degree of freedom for movement of the droplets.

The cover plate is comprised of ITO-coated glass with mechanically drilled ports for fluidic loading. A layer of photolithographically patterned polymer film sandwiched between the two plates is used to define the on-chip reservoirs, to seal the perimeter of the cartridge and to control the spacing between the two plates. The cover plate and PCB chip are coated with a proprietary hydrophobic coating and bonded with epoxy to complete the assembly of the fully enclosed, disposable PCR cartridge.

### Microfluidic Protocols

Prior to a PCR run, the cartridge is filled with a filler fluid. Either hexadecane or 2 cSt silicone oil was used, and the filler fluid was vacuum degassed first to prevent bubble generation during PCR (supporting information). Samples and reagents are pipetted into the cartridge through the fluidic loading ports and stored in the on-chip reservoirs. By switching proximate electrodes, droplets are aliquoted from the reservoirs with a unit volume

determined by the area of the dispensing electrode and the gap separating the top and bottom plates. The PCR cartridge has a unit electrode size of 1.1 mm × 1.1 mm and a gap height of 275 μm, providing consistent dispensing of droplets either 330 nl (i.e., single droplet) or 660 nl (i.e., double droplet) in volume depending on whether the droplet was formed across one or two electrodes. For a typical PCR assay, a single droplet of DNA sample and a single droplet of PCR master mix are separately dispensed from their reservoirs, mixed together, and the combined double droplet is then thermocycled between the two temperature zones. The electrode switching rate ranges from 4 to 16 Hz, providing a revolution period of 4 to 15 s for the droplet to travel through the entire PCR loop containing 58 electrodes. At the end of each cycle of annealing and extension, the droplet is transported to the detection electrode, and the fluorescence of the droplet is measured.

### PCR Chemistry

The following experimental conditions were used to evaluate the performance of the microfluidic PCR platform. The PCR mix contained 1× PCR buffer, 3 mM $MgCl_2$, 0.2 mM each of the dNTPs, 1 μM each of the primers and 0.5 unit/μl platinum *Taq* polymerase (Invitrogen, CA). The mix also included either 2× Eva Green (Biotium, CA) or 1 μM TaqMan® probe (Sigma-Aldrich, MO), depending on the target. Genomic DNA of methicillin-resistant *Staphylococcus aureus* (MRSA), *Candida albicans* and *Mycoplasma pneumoniae* were obtained from America Type Culture Collection (ATCC, MD) and prepared in biograde water with 0.1% Tween 20. The sequences of the primers and probe as well as the amplicon sizes are listed in Table S-1 (Supporting Information). The method used to calculate threshold cycle (Ct) numbers is also provided in Supporting Information.

## RESULTS AND DISCUSSION

### PCR Performance

The multi-channel PCR system was evaluated for real-time PCR detection of MRSA genomic DNA. A titration experiment using 10-fold dilutions of DNA samples ranging from 307 pg to 3.07 fg DNA input, which is equivalent of 100,000 to 1 MRSA genome copies, was performed to investigate the sensitivity of the system. The thermocycling conditions were 60 s hot-start at 95 °C, followed by 40 cycles of 10 s denaturation at 95 °C and 30 s annealing/extension at 60 °C. The real-time amplification results are shown in Figure 2.

The experiment was repeated three times on different chips. The average threshold cycle numbers and standard deviations were 14.52 ± 0.15, 17.90 ± 0.11, 21.24 ± 0.18, 24.78 ± 0.24, 27.81 ± 0.12, and 32.05 ± 1.67 for $10^5$, $10^4$,$10^3$,$10^2$, $10^1$, and $10^0$ genome equivalents, respectively. Following real-time PCR, droplets were collected from the chip and analyzed by gel electrophoresis (results not shown). The amplified products were of the expected length and no by-products were observed. The PCR amplification was highly reproducible as indicated by the small standard deviations of the Ct values. The larger standard deviation for the single-copy experiments is most likely due to the sampling variability at such low copy numbers. In other single-copy experiments the template was sometimes not detected as would be expected if the template were not present based on statistical sampling considerations. Nevertheless, the samples containing a single genome equivalent were amplified in a pattern consistent with the ability to detect a single organism within a sample droplet.

Linear regression of the average Ct values versus the logarithm of the amount of input DNA shows a slope of −3.4546 (Figure S-1, Supporting Information). The amplification efficiency of the PCR system, calculated using equation 1,

$$efficiency = 10^{-(1/slope)} - 1 \quad (1)$$

was 94.7%,[17] which is in the range of conventional bench-top thermocyclers and superior to most miniaturized flow-through PCR devices.[17]

## Optimization of PCR Speed

Ultra rapid PCR has been a goal for many of the miniaturized PCR devices. Miniaturization enables faster thermal cycling but dwell times may then become limited by reaction kinetics with further reductions in cycle time available only at the expense of reaction yield. We analyzed the kinetics of amplicon production at different stages of the 40-cycle PCR and developed a strategy to optimize both PCR speed and amplification efficiency. We used a method described by Neuzil *et al*[39] to monitor the increase in fluorescence within each annealing/extension cycle. For the $10^1$ dilution of MRSA with 10 s dwell at 95 °C and 30 s dwell at 60 °C, the Ct was 27.8. The fluorescence signal increases within cycles 26 through 30 and cycles 36 through 40 were measured and are shown in Figure 3A; these curves represent the exponential amplification phase and the saturation phase, respectively. For every cycle, there was an initial signal increase followed by a plateau from which we can estimate the actual time required to complete the extension of all amplicons in a particular cycle. These results clearly show that this completion time increased with the cycle number at the beginning of the exponential phase and then decreased when entering the saturation phase. Before the threshold cycle, 10 s appears sufficient to achieve full amplification for each cycle, likely due to the fact that the DNA template is present in small quantities compared to the excess reaction components. Considering this situation, the previous PCR was repeated with varying annealing/extension cycle times corresponding to the values required for reaction completion estimated from Figure 3A, which were 10 s for cycles 1 through 25, 30 s for cycles 26 through 35, and 20 s for cycles 36 through 40. The denaturation time was fixed at 6 s for all 40 cycles. The total annealing/extension time for this variable cycle time protocol was 650 s. A control experiment was also performed in which the same 650 s total annealing/extension time was achieved by dividing the total time evenly between all 40 cycles resulting in a fixed cycle time of 16 s.

The results of the three PCR protocols are shown in Figure 3B. Based on a comparison of the cycle threshold and reaction yield, PCR performance with varying cycle times was equivalent to the original 30 s fixed cycle time protocol, but the total annealing/extension time was reduced 46%. The control experiment with the same total reaction time achieved with a 16 s fixed cycle time had significantly reduced reaction yield, demonstrating the benefit of the variable cycle time protocol for faster PCRs.

With 6 s for denaturation and 4 s for droplet transport included in each variable cycle, the total time required to complete a 40 cycle PCR of MRSA genomic DNA with optimal reaction yield was 18 min. This result was obtained using platinum *Taq* polymerase (Invitrogen, CA) and could likely be improved through the use of faster polymerases, which are commercially available.[32]

The results demonstrate the feasibility of using digital microfluidics to optimize real-time PCR by using variable cycle times to adjust reaction conditions without sacrificing reaction efficiency. Practically, PCR amplification of an unknown sample can be managed using a “smart” software program that continuously monitors the fluorescence signal increase within each cycle and automatically triggers the next cycle once the signal reaches a plateau. Digital microfluidics is well-suited for this type of optimization because dwell times and

many other parameters can be dynamically recalibrated in real-time, which is impossible with less flexible formats.

## PCR Multiplexing

The digital microfluidic PCR cartridge can be configured to perform multiplexed PCR analysis by separating reactions in space rather than by spectral multiplexing: A DNA sample is loaded on the cartridge and divided into a set of sub-sample droplets, each of which is mixed with a droplet containing specific primer sets or probes in addition to PCR master mix. The number of sub-samples that can be generated from a single starting sample is virtually unlimited but the sensitivity is potentially reduced each time the sample is sub-divided. All of the droplets are circulated within a single common loop and sequentially passed through the same detection site allowing analysis of multiple genetic targets in a single DNA sample. The four individual loops can be used to achieve multi-target PCR analysis of up to four different DNA samples in parallel, thereby adding another level of multiplexing. In principle, reporters with multiple different wavelengths could also be employed in each droplet to further increase multiplexing but the current experimental setup uses only a single wavelength detector. As a conceptual demonstration, a multichannel two-plex PCR assay was conducted with the following DNA sample configuration: sample A (loop 1), 1.6 pg/μl MRSA DNA; sample B (loop 2), 1.6 pg/μl *M. pneumoniae* DNA; sample C (loop 3), 1.6 pg/μl MRSA DNA and 1.6 pg/μl *M. pneumoniae* DNA.

The cartridge was programmed to initially distribute a single (i.e., 330 nl) droplet of PCR mix containing MRSA primers to each loop from a common reagent reservoir, followed by a single droplet of PCR mix containing *M. pneumoniae* primers. Next, two single droplets were dispensed from each DNA sample reservoir, transported to the loop and combined with each of the two previously distributed PCR mix droplets containing MRSA or *M. pneumoniae* primers. The two-plex real-time PCR was then conducted by circulating the two combined double droplets in each loop and passing each droplet through the detection site once per cycle. All of the DNA targets in the three samples were successfully detected with no false positive results and the threshold cycles were comparable with the single-plex PCR. The results are shown in Figure 4.

A common problem for microchip PCR is the non-specific adsorption of DNA molecules to the chip surface, which can be mitigated by various means but remains difficult to completely eliminate. Loss of DNA to chip surfaces can result in reduced sensitivity as well as cross-contamination between samples traveling through shared pathways. Even one DNA template inadvertently transferred between samples can be exponentially amplified and result in a false positive result. This is particularly likely to occur if different samples are amplified serially because even the carry-over of 1 part per billion from a completed reaction can contaminate the next reaction. For this reason, the digital microfluidic PCR chips are intended to be used once and discarded, which is economically feasible due to their low cost PCB construction. Additionally, the chips are designed so that the pathways of droplets from different samples never intersect. In the multiplex PCR experiment, all of the droplets that were circulated in a common loop originated from the same DNA sample so cross-contamination of the samples was not a concern. The possibility of carry-over of primers, amplicons or reporters between reactions exists but these contaminants are not exponentially amplified in the reaction. As confirmed by the negative controls in the two-plex experiment (negative droplet #2 in loop 1 and negative droplet #1 in loop 2), this form of contamination may not be significant. In these experiments different DNA samples were simultaneously amplified in separate loops located within a common reservoir of oil. Although the filler oil could potentially provide another route for cross-contamination, this problem was not observed in these experiments. We have therefore demonstrated the

feasibility of combined spatial and time-division multiplexing which can significantly increase the assay throughput of the digital microfluidic PCR system.

### Manipulation of Beads

Paramagnetic beads are commonly used in biological and clinical assays to capture or immobilize targets of interest such as DNA, RNA, whole cells, or specific antigens or antibodies. They also provide a convenient means for concentrating these targets and transferring them between different liquid media. Figure 5 illustrates a process for concentrating paramagnetic beads from a sample volume of 5--10 μl into a single 330 nl droplet using a permanent magnet embedded in the cartridge deck. By design, the magnetic field is strong enough to concentrate the beads within the liquid body and permit liquid exchange, but not strong enough to pull the beads through the oil-water interface at the droplet meniscus. Therefore, when the droplet is transported away from the position of the magnet the beads are retained inside the droplet and when removed from the magnetic field the beads become quickly resuspended due to the intrinsic fluid circulation within a moving droplet. This concentration technique enables larger specimen volumes to be analyzed in microfluidic volumes without loss of sensitivity.

However, fluorescence background measurements were considerably noisier when relatively high concentrations of magnetic beads where present in the droplet. This artifact was presumably due to the effect of light scattering from randomly distributed beads. To address this problem, an additional magnet was embedded in the cartridge deck in proximity to the detection spot on the PCR cartridge. As the droplet approaches the detection spot this magnet causes the beads to be pulled towards one edge of the droplet clarifying the illuminated center of the droplet. The effect of this additional magnet can be clearly seen in Figure 6 where identical PCR experiments including magnetic beads were performed with and without this external magnet in place.

### PCR Analysis of Realistic Samples

The capability to perform sample concentration and solution exchange (i.e., washing and/or elution) on-chip using magnetic beads makes this device suitable for the detection of DNA of pathogens that are normally present in low concentrations in actual clinical specimens. To demonstrate this capability, we tested the PCR system using simulated clinical samples. Human whole blood was spiked with *Candida albicans* (ATCC 36082) yeast cells at a concentration of $10^3$/mL, negative controls consisted of human blood lacking *C. albicans*, and all were processed using a bead-based DNA extraction and purification protocol.[40] The microbial DNA was captured on paramagnetic beads (Dynabeads®, Invitrogen, CA) using an oligonucleotide capture probe and suspended in 6 μl TE buffer as the sample inputs for the PCR cartridge. The detection chemistry utilized a DNA sequence-specific TaqMan® probe and 2 cSt silicone oil was used as the filler fluid. Amplification of the *C. albicans* DNA from the simulated clinical beads sample was successful and the result is shown in Figure S-2, Supporting Information.

## CONCLUSION AND OUTLOOK

We successfully developed a multiplexed real-time PCR system using electrowetting-based digital microfluidics. The system exhibited remarkable amplification efficiency of 94.7% and detected the equivalent of a single genome for a methicillin-resistant *Staphylococcus aureus* (MRSA) model test system. Parallel two-plex PCR amplification of multiple DNA samples was demonstrated as proof-of-principle for high-throughput multiplexed PCR applications. The “smart” cycle time management proposed in this work, coupled with the rapid thermocycling capability made possible by digital microfluidics, provides a promising

solution to dramatically reduce the PCR time without compromising reaction yield. This versatile system also accommodates magnetic bead handling capability which was applied to analyze simulated clinical samples prepared from whole blood using a magnetic bead capture protocol. The experiments using target DNA from *S. aureus*, *M. pneumoniae* or *C. albicans* demonstrate the potential application of the microfluidic PCR system to detect microbial DNA in clinical specimens for the rapid diagnosis of infectious diseases.[40]

The reproducibility and sensitivity of the digital microfluidic PCR system presented here compares favorably to conventional bench-top real-time PCR instruments but provides many advantages in terms of automation, cost and time-to-result. The design of the PCR cartridge is highly modular enabling it to be scaled-up for high throughput applications or combined with other modules to meet application-specific demands. Although the work reported here used a two-heater configuration, it is straightforward to integrate additional heaters for three temperature PCR, RT-PCR or other processes. The dramatically reduced sample volume, reagent costs and assay turn-around time, as well as the user-friendly interface make the system a promising platform for routine PCR assays in a research or clinical laboratory.

The electrically enabled fluidic manipulation avoids the need for bulky mechanical pumps and valves. Power consumption is minimized because thermocycling of heaters is avoided in the flow-through approach and because electrowetting is inherently low-power. The digital microfluidic PCR system is therefore well-suited for further miniaturization as a portable device platform for rapid point-of-care tests and field applications, which are beyond the reach of conventional PCR instruments.

The digital microfluidic platform offers a high degree of assay configurability. A single generic chip can be configured in software to implement a wide range of assays and protocols using a common library of basic droplet operations. The flexibility and breadth of digital microfluidics combined with thermocycling and bead manipulation capability enables the integration of PCR amplification with other pre-PCR or post-PCR processes for complete “sample to answer” automation.

## Supplementary Material

Refer to Web version on PubMed Central for supplementary material.

## Acknowledgments

The authors gratefully acknowledge the technical contributions of Ryan Sturmer and Greg Smith of Advanced Liquid Logic. This work was partially support by a NIH grant (U01 AI 066590).

## References

1. Kricka LJ, Wilding P. Anal Bioanal Chem 2003;377:820–825. [PubMed: 12925867]
2. Roper MG, Easley CJ, Landers JP. Anal Chem 2005;77:3887–3894. [PubMed: 15952761]
3. Lagally ET, Emrich CA, Mathies RA. Lab Chip 2001;1:102–107. [PubMed: 15100868]
4. Ottesen EA, Hong JW, Quake SR, Leadbetter JR. Science 2006;314:1464–1467. [PubMed: 17138901]
5. Giordano B, Ferrance J, Huhmer AFR, Swedberg S, Landers JP. Anal Biochem 2001;291:124–132. [PubMed: 11262165]
6. Kopp MU, deMello J, AJ, Manz A. Science 1998;280:1046–1048. [PubMed: 9582111]
7. Obeid PJ, Christopoulos TK, Crabtree HJ, Backhouse CJ. Anal Chem 2003;75:288–295. [PubMed: 12553764]
8. Schneegaβ I, Bräutigam R, Köhler JM. Lab Chip 2001;1:42–49. [PubMed: 15100888]

9. Easley CJ, Humphrey JAC, Landers JP. J Micromech Microeng 2007;17:1758–1766.
10. Dorfman KD, Chabert M, Codarbox JH, Rousseau G, de Cremoux P, Viovy JL. Anal Chem 2005;77:3700–3704. [PubMed: 15924408]
11. Curcio M, Roeraade J. Anal Chem 2003;75:1–7. [PubMed: 12530811]
12. Beer NR, Hindson BJ, Wheeler EK, Hall SB, Rose KA, Kennedy IM, Colston BW. Anal Chem 2007;79:8471–8475. [PubMed: 17929880]
13. Schaerli Y, Wootton RC, Robinson T, Stein V, Dunsby C, Neil MAA, French PMW, deMello AJ, Abell C, Hollfelder F. Anal Chem 2009;81:302–306. [PubMed: 19055421]
14. Ohashi T, Kuyama H, Hanafusa N, Togawa Y. Biomed Microdevices 2007;9:695–702. [PubMed: 17505884]
15. Pipper J, Inoue M, Ng LFP, Neuzil P, Zhang Y, Novak L. Nat Med 2007;13:1259–1263. [PubMed: 17891145]
16. Sun Y, Kwok YC, Nguyen NT. Lab Chip 2007;7:1012–1017. [PubMed: 17653343]
17. Chen L, West J, Auroux PA, Manz A, Day PJR. Anal Chem 2007;79:9185–9190. [PubMed: 17979297]
18. Wang W, Li ZX, Luo R, Lü SH, Xu AD, Yang YJ. J Micromech Microeng 2005;15:1369–1377.
19. Liu J, Enzelberger M, Quake S. Electrophoresis 2002;23:1531–1536. [PubMed: 12116165]
20. Frey O, Bonneick S, Hierlemann A, Lichtenberg J. Biomed Microdevices 2007;9:711–718. [PubMed: 17505882]
21. Pollack MG, Fair RB, Shenderov AD. Appl Phys Lett 2000;77:1725–1726.
22. Lee J, Moon H, Fowler J, Schoellhammer T, Kim CJ. Sens Actuators, A 2002;95:259–268.
23. Pollack MG, Fair RB, Shenderov AD. Lab Chip 2002;2:96–101. [PubMed: 15100841]
24. Cho SK, Moon HJ, Kim CJ. J Microelectromech Syst 2003;12:70–80.
25. Mugele F, Baret JC. J Physics-Condensed Matter 2005;17:705–774.
26. Fouillet Y, Achard JL. Comptes Rendus Physique 2004;5:577–588.
27. Wheeler AR. Science 2008;322:539–540. [PubMed: 18948529]
28. Srinivasan V, Pamula VK, Fair RB. Anal Chim Acta 2004;507:145–150.
29. Paik P, Pamula VK, Fair RB. Lab Chip 2003;3:253–259. [PubMed: 15007455]
30. Fair RB. Microfluid Nanofluid 2007;3:245–281.
31. Fouillet Y, Jary D, Chabrol C, Claustre P, Peponnet C. Microfluid Nanofluid 2008;4:159–165.
32. Sista R, Hua Z, Thwar P, Sudarsan A, Srinivasan V, Eckhardt A, Pollack M, Pamula V. Lab Chip 2008;8:2091–2104. [PubMed: 19023472]
33. Miller EM, Wheeler AR. Anal Chem 2008;80:1614–1619. [PubMed: 18220413]
34. Moon H, Wheeler AR, Garrell RL, Loo JA, Kim CJ. Lab Chip 2006;6:1213–1219. [PubMed: 16929401]
35. Chang YH, Lee GB, Huang FC, Chen YY, Lin JL. Biomed Microdevices 2006;8:215–225. [PubMed: 16718406]
36. Fouillet, Y.; Jary, D.; Brachet, AG.; Berthier, J.; Blervaque, R.; Davoust, L.; Roux, JM.; Achard, JL.; Peponnet, C. Proc. ASME ICNMM; 2006.
37. Paik PY, Allen DJ, Eckhardt AE, Pamula VK, Pollack MG. Proc Micro Total Analysis Systems (μTAS) 2007:1559–1561.
38. Hua Z, Allen DJ, Thwar P, Eckhardt AE, Pamula VK, Pollack MG. Proc Micro Total Analysis Systems (μTAS) 2008:1713–1715.
39. Neuzil P, Zhang C, Pipper J, Oh S, Zhuo L. Nucleic Acids Res 2006;34:e77. [PubMed: 16807313]
40. Wulff-Burchfield, E.; Schell, WA.; Eckhardt, AE.; Pollack, MG.; Hua, Z.; Rouse, JL.; Pamula, VK.; Srinivasan, V.; Benton, JL.; Alexander, BD.; Wilfret, DA.; Kraft, M.; Cairns, C.; Perfect, JR.; Mitchell, TG. Diagnostic Microbiology and Infectious Diseases (accepted).

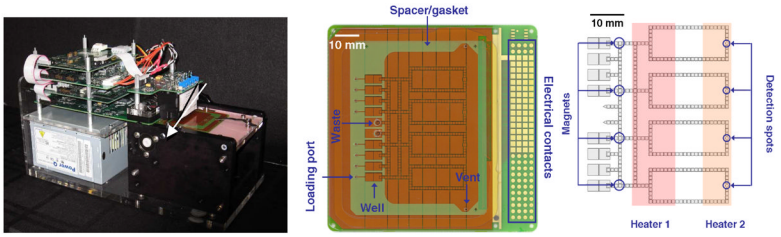


(A) (B) (C)

**Figure 1.**

Self-contained digital microfluidic PCR system. (A) The instrument including power supply, control electronics, fluorimeter module, heaters and cartridge deck (shown with cartridge loaded). (B) Photograph of assembled microfluidic cartridge comprising a PCB chip, polymer spacer/gasket and glass top-plate with drilled holes. (C) Schematic of PCR chip showing electrode positions relative to heaters, magnets and detectors.

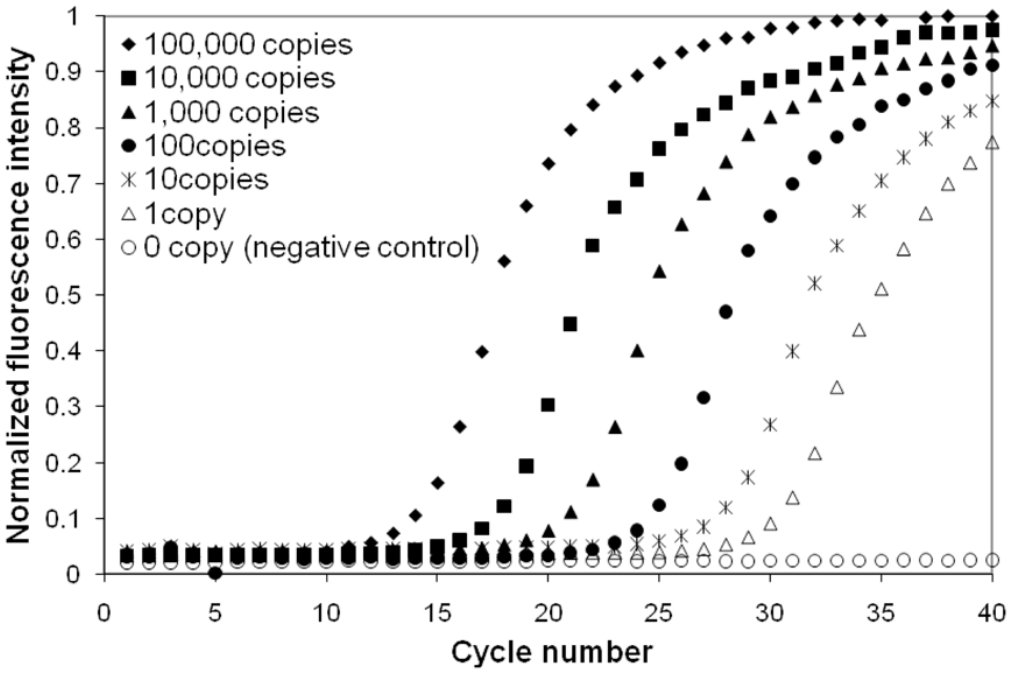


**Figure 2.**
PCR titration experiment using 10-fold serial dilutions of MRSA genomic DNA on the digital microfluidic PCR platform. The DNA inputs were 1 to 100,000 genomic equivalents and the negative control.

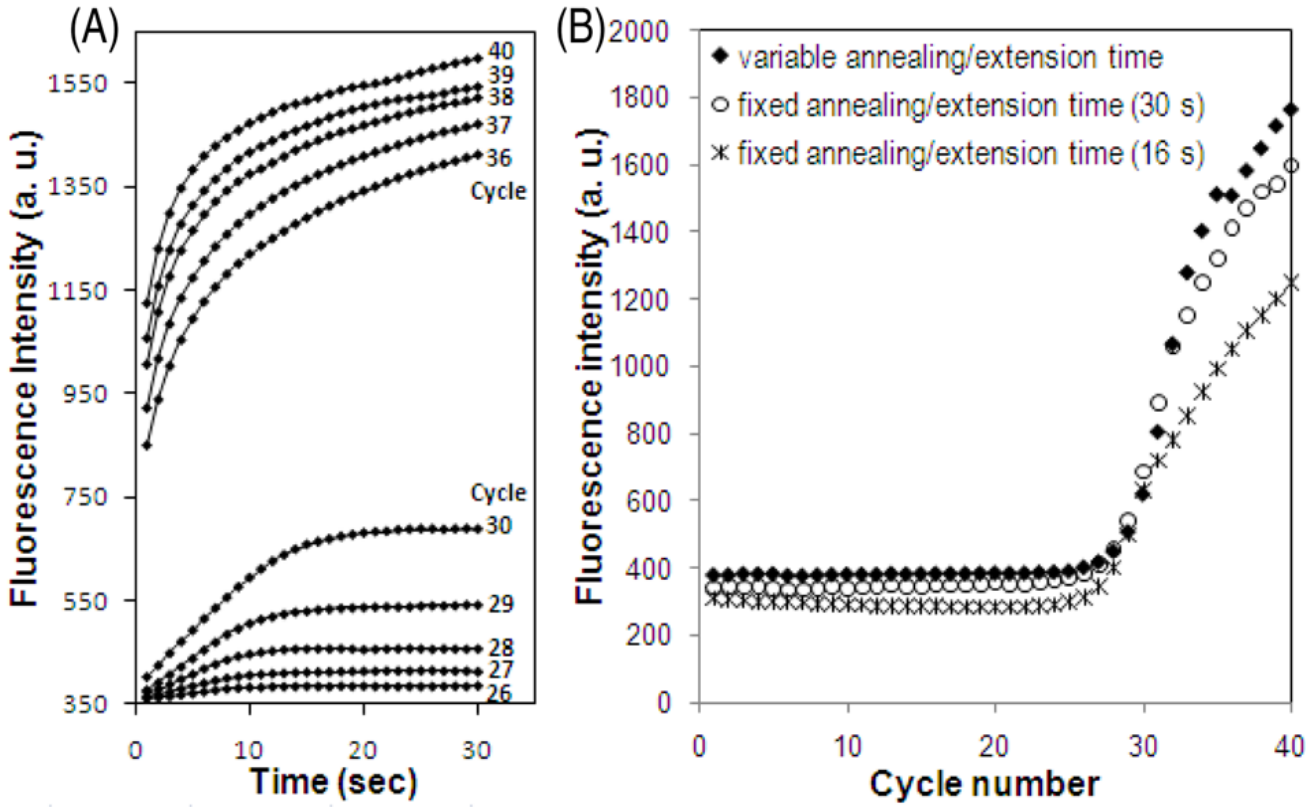


**Figure 3.**

Real-time PCR using fixed and variable cycle times. Other conditions were identical for all the reactions. The input template was 30.7 fg MRSA genomic DNA. (A) Fluorescence signal increase within each PCR annealing/extension cycle (measured once per second over 30 seconds) for a real-time PCR consists of 2 min at 95 °C followed by 40 cycles of 10 s denaturation at 95 °C and 30 s annealing/extension at 60 °C. (B) Comparison of fixed and variable cycle time protocols. The two fixed cycle time protocols consisted of 10 s (6 s) denaturation and 30 s (16 s) annealing/extension throughout 40 cycles. The variable cycle time protocol consisted of 6 s denaturation throughout 40 cycles, and annealing/extension of 10 s for cycles 1 through 25, 30 s for cycles 26 through 35 and 20 s for cycles 36 through 40.

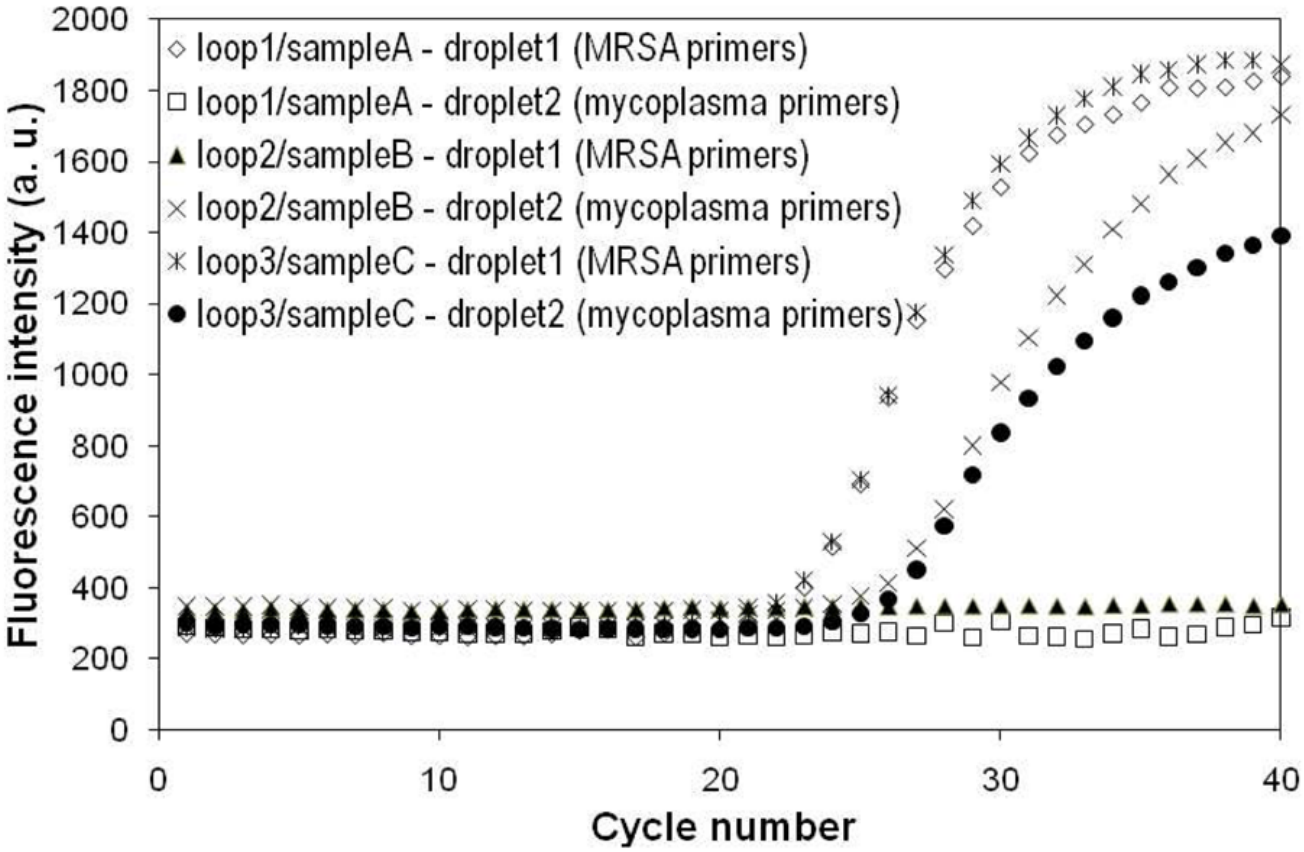


**Figure 4.**

Two-plex (MRSA and *M. pneumoniae*) real-time PCR assay of three different DNA samples in parallel on the digital microfluidic PCR platform. The PCR conditions were 60 s hot-start at 95 °C followed by 40 cycles of 10 s denaturation at 95 °C and 30 s annealing/extension at 60 °C. Loop1/sample A contained only MRSA template DNA; loop2/sample B, only *M. pneumoniae* template; and loop3/sample C contained both templates.

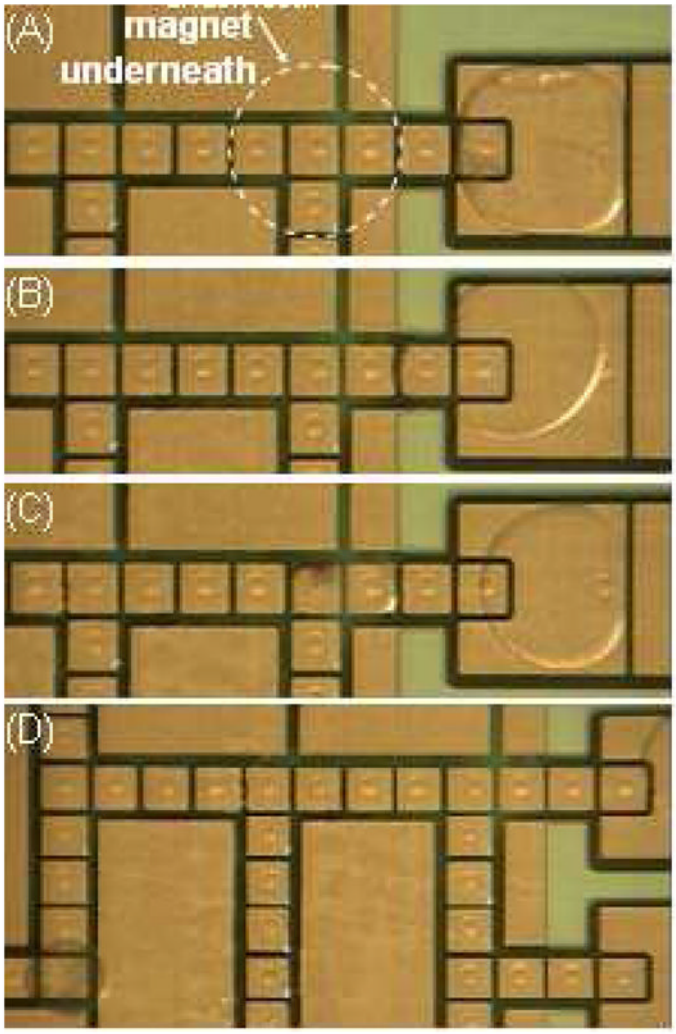


**Figure 5.**

Concentrating paramagnetic beads from a 5 μl sample to a nanoliter droplet. (A) Beads (5 μg/μl) in the sample migrate towards the magnet and aggregate at the interface. (B) A liquid finger is pulled from the sample and all the beads stay at the front edge of the finger. (C) A 660 nl droplet is dispensed and contains all the beads from the sample in the reservoir. (D) The droplet containing beads moves away from the magnet position and the beads are re-dispersed.

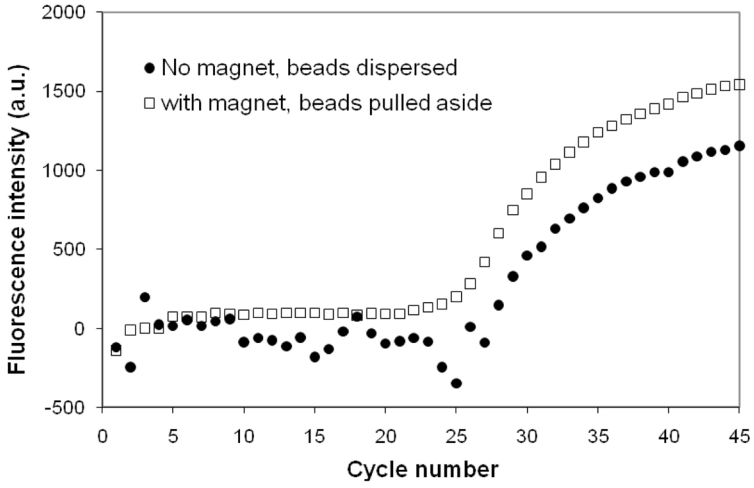


**Figure 6.**
Effects of the external magnet on fluorescence readings for a real-time PCR with 2.5 μg Dynabeads (Invitrogen, CA) added to the 660 nl reaction droplet.